Journal of Vibration Engineering & Technologies (2023) 11:3081–3092
https://doi.org/10.1007/s42417-022-00732-4

ORIGINAL PAPER

Energy Regeneration Effects on the Vehicle Suspension System Performance Considering Non-idealities

Omid Kavianipour[1]

Received: 15 May 2022 / Revised: 27 September 2022 / Accepted: 29 September 2022 / Published online: 11 October 2022
© Krishtel eMaging Solutions Private Limited 2022

Abstract

Introduction Electromagnetic dampers, that are composed of a permanent-magnet DC motor, a ball screw, and a nut, are one of the devices currently being inspected to regenerate energy from the vehicle suspension system. In view of that, this research paper focuses on developing mathematical model for an energy storage system in conjunction with the electromagnetic damper for the sake of energy regeneration of the vehicle suspension system.

Methods The energy storage system considered herein comprises of a unidirectional converter, a full wave rectifier, and an ultracapacitor stack. Some of non-idealities that affect the act of the converter are considered for modeling of the energy storage system. Subsequently, the vehicle suspension system performance analysis along with energy regeneration is carried out based on the developed mathematical model and the role of resistance R (design parameter) in the electric circuit on the vehicle suspension system performance is revealed. Furthermore, considering the variable resistance, a simple method to adjust the parameter of the continuous skyhook control strategy for the semi-active electromagnetic suspension system is proposed in this paper.

Results The simulation results demonstrate that the designed semi-active electromagnetic suspension system has the better performance and more energy regeneration than the passive electromagnetic suspension system.

Keywords Energy regeneration · Vehicle suspension system · Electromagnetic damper · Ultracapacitor · Unidirectional converter

Introduction

The main tasks of vehicle suspension system are to support the vehicle body weight, to isolate the vehicle chassis from road disturbances, and to force the wheels to keep the road surface. In other words, any suspension system functions to compromise two main contradictory factors, i.e., ride comfort and handling stability. The vehicle body acceleration and suspension travel affect the ride comfort and handling stability, respectively. Two key elements in a conventional suspension system are the spring and damper. This kind of suspension system leads to dissipate vibration energy into heat to decrease the vibration transmitted by road excitation. On the other hand, nowadays, researchers and engineers are paying more attention to electric vehicles and hybrid electric vehicles since the fuel consumption is decreased and as a result, air pollution is reduced. Due to the energy storage systems such as fuel cells, batteries, ultracapacitors, and superconducting magnetic energy storage systems, these vehicles provide the ability of energy regeneration in the vehicle subsystems. Therefore, the conditions of harvesting the suspension system energy have been prepared. In this direction, several types of regenerative suspension systems have been developed recently that are still in the stage of investigation.

Zhang et al. [1] proposed an electromagnetic shock absorber applying a rack and pinion mechanism. The efficiency of this device is typically high, however, its damping coefficient is small relatively. In addition, Tang et al. [2] designed a linear vibration energy regenerator with an efficiency about 70 percent and the maximum damping coefficient around 940 Ns/m. Gysen et al. [3] offered a suspension system which can both deliver active force and regenerate power because of enforced movements. Despite considering a linear quadratic regulator controller for the progress

✉ Omid Kavianipour
o.kavianipour@damavandiau.ac.ir

[1] Department of Mechanical Engineering, Damavand Branch, Islamic Azad University, Damavand 3971878911, Iran

of comfort and handling, the damping coefficient was too small, although this prototype mechanism had high efficiency. Kawamoto [4] evaluated the performance of the electro-mechanical ball screw shock absorber, which is designed in order to increase the damping coefficient, on the energy consumption, vibration isolation, and vehicle handling. An energy-harvesting suspension system using ball screws was proposed in [5] and attained a damping coefficient between 3200 and 7400 Ns/m and an efficiency between 41 and 81 percent. Roshan [6] manufactured a mechanism with two legs so as to change translational motion into rotary motion. The characteristics of this energy-regenerative damper were a damping coefficient of 650 Ns/m and the efficiency between 73 and 84 percent. Zhang et al. [7] suggested a regenerative shock absorber comprising a pair of gear rack structures and supercapacitors that converts irregularly reciprocating linear vibration into unidirectional rotation. Rotating in one direction can increase the efficiency of the energy-harvesting suspension system. Salman et al. [8] proposed a regenerative shock absorber using helical gears and dual tapered roller clutches. The average efficiency of this shock absorber is nearly 40 percent when the vibration amplitudes and the frequencies vary from 1 to 5 mm and 1 to 2.5 Hz, respectively. Liu et al. [9] manufactured an energy harvester mechanism utilizing a ball screw and two overrun clutches with an efficiency between 41 and 65 percent in 7.5 mm excitation. Zhang et al. [10] designed a regenerative suspension system based on the arm-teeth mechanism which is able to convert linear movement to rotary motion indirectly.

Galluzzi [11] proposed a hydraulic regenerative suspension system which change the linear movement into angular motion. In spite of the improvement of the energy conversion efficiency, the damping control property is not affected in this system. Zhang et al. [12] showed that the average output power of the hydraulic electromagnetic semi-active suspension system can reach to 110.6 W with an excitation speed of 0.52 m/s. Fang et al. [13] presented an electro-hydraulic damper which can recover energy approximately 200 W at the excitation with a frequency of 10 Hz and largeness of 3 mm. Abdelkareem et al. [14] investigated the harvesting vibration energy from heavy-duty truck suspension system. They showed that the average power of 300 W can be regenerated when the truck speed is 60 mph on the road grade D. A comprehensive review on regenerative shock absorber systems based on vehicle suspensions is performed in [15] and [16].

It should also be taken into account that regenerative shock absorbers necessitate efficient and reliable energy storage systems. Among different types of energy storage systems, ultracapacitors have high reliability, fast charging and discharging speed, long cycle life, and low-maintenance [17–20]. For this reason, ultracapacitors are utilized in the automobile industries, especially in electric vehicles [21–24]. In addition, a hybrid energy storage system including the ultracapacitor and battery makes a better choice in pulsed load currents applications [25]. The energy losses in a hybrid energy storage system assuming equivalent series resistance is investigated in [26]. A power management control in the hybrid energy storage system for electric vehicles is studied in [27]. A Li-ion ultracapacitor using an electrical equivalent circuit is inspected in [28]. Bharti et al. [29] reviewed the modeling techniques and simplified analytical models suggested for the theoretical study of supercapacitors considering their limitations. Navarro et al. [30] described the use of ultracapacitor technology and the control strategies in the industrial applications. It is to be noted that most energy storage systems have numerous ultracapacitors attached in series and parallel called ultracapacitor stack. Moreover, using a converter along with ultracapacitor stack is suitable for keeping a stiff voltage at the terminals of the ultracapacitor stack [31].

Contributions: Considering the advantages of ball screw shock absorbers and ultracapacitors mentioned earlier, the electromagnetic suspension system is considered to be analyzed in this research paper. This system consists of two main parts: (1) the electromagnetic damper including a permanent-magnet DC motor, a ball screw and a nut and (2) the energy storage system including a unidirectional converter, a full wave rectifier, and an ultracapacitor stack. The basic objective of this work is to develop a more accurate mathematical model by considering some non-ideal cases for the proper design of an electromagnetic suspension system. In this regard, the effect of the substantial design parameter, i.e., the resistance R on the vehicle suspension system performance is revealed. In addition, a simple method to adjust the parameter of the continuous skyhook control strategy for the semi-active electromagnetic suspension system is suggested in order to improve the performance and the harvested energy of the vehicle suspension system. The simulation results show that the best RI is 0.511 m/s^2 when R is 3.4 Ω in dissipation mode and the best RI is 0.510 m/s^2 when R is 3.3 Ω in regeneration mode. After crossing the bump, 5.5 s are approximately required that the vibration of the suspension system becomes zero and in this conditions, the state of charge is reached to 0.21 v. The results demonstrate that the passive and semi-active electromagnetic suspension systems are able to regenerate energy up to 7.6 and 8.6 J/s in 80 s, respectively, when crossing an almost rough road. The structure of this paper is as follows.

In "Mathematical Modeling", the non-linear state space equations of the system are extracted based on the features of quarter vehicle model, ball screw shock absorber, electric circuit of DC motor, converter, rectifier, and ultracapacitor stack. Hereof, non-idealities considered in this work are associated with the converter. The effects of the resistance

R on the performance of the vehicle suspension system in terms of ride comfort and maximum suspension travel in the dissipation and regeneration modes are evaluated in "Investigation of the Resistance R role". "Simulation Results" pays attention to energy regeneration process of the electromagnetic suspension system when passing through a bump by the use of simulation results. Moreover, this section deals with the comparison of the passive and semi-active electromagnetic suspension systems in aspect of harvesting energy and performance when passing through a random road profile.

Mathematical Modeling

Electromagnetic Suspension System

The car model based on the two degrees of freedom demonstrated in Fig. 1 is the most current model in the design studies for the vehicle suspension systems. Having regenerative ball screw shock absorbers, these types of suspension systems are entitled electromagnetic suspension systems. The ball screw mechanism can transform the linear motion of the vehicle vibration into rotary motion as an input torque for the DC motor. Consequently, the generated force has the role of damping force in the vehicle suspension system.

Applying Newton's second law, the equations of the electromagnetic suspension system may be achieved as follows:

$$\begin{aligned} -k_s\left(y_s-y_u\right)+f &= m_s\ddot{y}_s \\ k_s\left(y_s-y_u\right)-f-k_t\left(y_s-y_g\right) &= m_u\ddot{y}_u \end{aligned} \tag{1}$$

where k_s is the spring stiffness of the suspension system spring, k_t is the spring stiffness of the tire, m_s is the sprung mass, m_u is the unsprung mass, y_s is the body displacement, y_u is the wheel displacement, $\ddot{y}_s$ is the sprung mass acceleration, $\ddot{y}_u$ is the unsprung mass acceleration, and y_g is the road input. The electromagnetic damper force, i.e., f, was modeled by Kawamoto et al. [32] and is in the form of

$$f = -\varphi\, i - c_e\left(\ddot{y}_s-\ddot{y}_u\right)-I\left(\ddot{y}_s-\ddot{y}_u\right) \tag{2}$$

where φ is the motor constant, i is the current of the motor circuit, c_e is the equivalent damper coefficient, I is the equivalent inertia, $\dot{y}_s$ is the sprung mass velocity, and $\dot{y}_u$ is the unsprung mass velocity. The parameter values of a typical car model and the electromagnetic damper are presented in Table 1 [32].

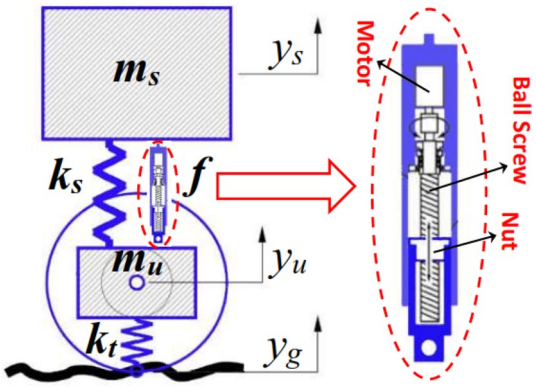

Fig. 1 Electromagnetic regenerative suspension system including a motor, a ball screw and a nut

Energy Storage System

In Fig. 2, the energy storage system proposed to store regenerative energy from vehicle vibrations is shown in details. This system consists of a unidirectional converter, a full wave rectifier, and an ultracapacitor stack. The equivalent DC motor circuit including the resistance (r_m) and the inductance (L_m) is considered for modeling of the motor of the electromagnetic damper. In converters, metal oxide semiconductor field effect transistor (MOSFET) is popular for power electronic system applications involving low-power and high-frequency switching applications [31]. The well-known non-idealities related to the MOSFET-based converter are the ON-state resistance of the switches (r_{s1} and r_{s2}), ON-state voltage drop of the switches which is minimal in contrast with the drop caused by ON-state resistance and thus can be neglected, and the parasitic resistance (r_c) of the filter inductor (L_c). The design parameter, i.e., the constant/variable resistance R that impacts on the energy regeneration amount and the vehicle suspension system performance is taken into consideration in this work. Assuming the ideal diodes, there is no need to augment any resistances in the rectifier circuit. The equivalent circuit of the ultracapacitor stack which estimates its non-ideal behavior consists of the equivalent series resistance (*ESR*) and equivalent parallel resistance (*EPR*). Typically, the value of *EPR* is very high and the value of *ESR* is very low and thus can be neglected.

Table 1 The parameter values of the electromagnetic suspension system

Parameter	Value
m_s (kg)	344
m_u (kg)	40
k_s (N/m)	20,053
k_t (N/m)	182,087
Φ (N/A)	66
c_e (Ns/m)	20
I (kg)	18
r_m (Ω)	1.16
L_m (H)	0.002

The parameters values of the energy storage system are given in Table 2 [31].

According to [32], the induced voltage of the motor in the electric circuit is equal to

$$v_m = \varphi\left(\dot{y}_s - \dot{y}_u\right) \tag{3}$$

When the value of the induced voltage of the motor is greater than the ultracapacitor stack voltage, the electromagnetic damper can regenerate the vibration energy and this state is named as the regeneration mode. However, when the amount of the induced voltage of the motor is less than the ultracapacitor stack voltage, the electromagnetic damper is not able to transfer energy to the ultracapacitor stack. This state is named as the dissipation mode. In practice, the values of the induced voltage of the motor and the ultracapacitor stack voltage are measured using voltage sensors. Based on the voltage comparison, the appropriate command for opening or closing the switches and relays is then run by the control unit.

Therefore, the two modes in which the converter operates are a) dissipation mode (during which switch sw_1 is ON and switch sw_2 is OFF) and b) regeneration mode (during which switch sw_2 is ON and switch sw_1 is OFF). By means of Kirchhoff's voltage law, the differential equations describing the converter behavior in these two modes can be written as

(a) Dissipation mode

$$\begin{aligned} v_m &= \left(r_m + R + r_{s1}\right)i + L_m\dot{i} \\ \dot{v}_u &= 0 \end{aligned} \tag{4}$$

(b) Regeneration mode

$$\begin{aligned} v_m &= \left(r_m + R + r_{s2} + r_c\right)i + \left(L_m + L_c\right)\dot{i} + v_u \\ \dot{v}_u &= \frac{1}{c_u}|i| \end{aligned} \tag{5}$$

where R is the resistance whose value is assigned by the designer, c_u is the capacitance of the ultracapacitor stack, and v_u is the ultracapacitor stack voltage.

By introducing the parameter d which is equal to 0 in dissipation mode or 1 in regeneration mode, Eqs. (4) and (5) can be mixed as follows:

$$\begin{aligned} v_m &= \left(r_m + R + (1-d)r_{s1} + d\left(r_{s2} + r_c\right)\right)i + \left(L_m + dL_c\right)\dot{i} + dv_u \\ \dot{v}_u &= \frac{d}{c_u}|i| \end{aligned} \tag{6}$$

The state space model of the whole system is of special importance to make a design framework. Therefore, considering Eqs. (1), (2), (3), (6), and the state variables in the following form:

$$\left\{x_1 = y_s, x_2 = \dot{y}_s, x_3 = y_u, x_4 = \dot{y}_u, x_5 = i, x_6 = v_u\right\} \tag{7}$$

the state space model of the electromagnetic suspension system along with the energy storage system is obtained as

$$\begin{aligned}
\dot{x}_1 &= x_2 \\
\dot{x}_2 &= \left(\frac{-m_u k_s}{m_s m_u + Im_u + Im_s}\right)x_1 + \left(\frac{-m_u c_e}{m_s m_u + Im_u + Im_s}\right)x_2 \\
&\quad + \left(\frac{m_u}{m_s m_u + Im_u + Im_s}(k_s - I\frac{k_t}{m_u})\right)x_3 + \left(\frac{m_u c_e}{m_s m_u + Im_u + Im_s}\right)x_4 \\
&\quad + \left(\frac{-m_u \varphi}{m_s m_u + Im_u + Im_s}\right)x_5 + \left(\frac{m_u}{m_s m_u + Im_u + Im_s}\left(I\frac{k_t}{m_u}\right)\right)y_g \\
\dot{x}_3 &= x_4 \\
\dot{x}_4 &= \left(\frac{m_s k_s}{m_s m_u + Im_u + Im_s}\right)x_1 + \left(\frac{m_s c_e}{m_s m_u + Im_u + Im_s}\right)x_2 \\
&\quad + \left(\frac{-m_s}{m_s m_u + Im_u + Im_s}\left(k_s - I\frac{k_t}{m_u}\right) - \frac{k_t}{m_u}\right)x_3 + \left(\frac{-m_s c_e}{m_s m_u + Im_u + Im_s}\right)x_4 \\
&\quad + (\frac{m_s \varphi}{m_s m_u + Im_u + Im_s})x_5 + (\frac{-m_s}{m_s m_u + Im_u + Im_s}(I\frac{k_t}{m_u}) + \frac{k_t}{m_u})y_g \\
\dot{x}_5 &= \left(\frac{\varphi}{L_m + dL_c}\right)x_2 + \left(\frac{-\varphi}{L_m + dL_c}\right)x_4 \\
&\quad + \left(-\frac{r_m + R + (1-d)r_{s1} + d(r_{s2} + r_L)}{L_m + dL_c}\right)x_5 \\
&\quad + \left(\frac{-d}{L_m + dL_c}\right)x_6\dot{x}_6 = \left(\frac{d}{c_u}\right)|x_5|
\end{aligned} \tag{8}$$

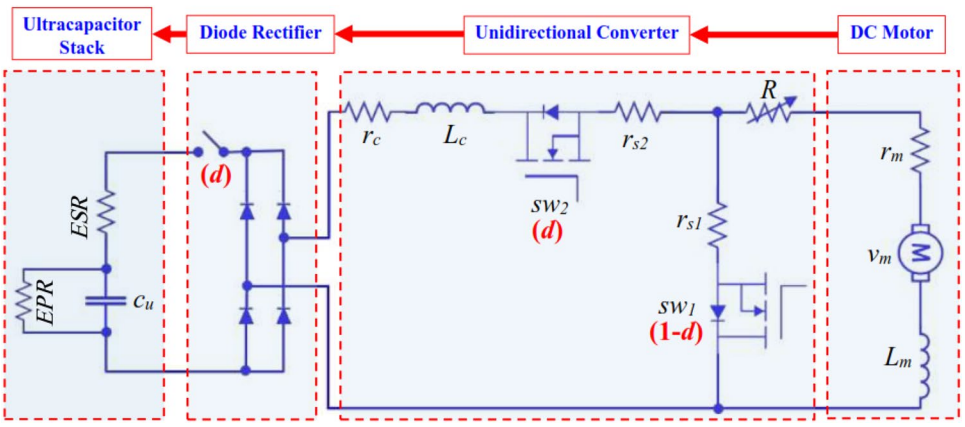

Fig. 2 Circuit diagram of the energy storage system for the electromagnetic damper including a converter, a rectifier and an ultracapacitor stack

Investigation of the Resistance *R* role

Transfer Functions

The state space equations given by Eq. (8) are non-linear for existence of the parameter d in the equations. As shown in [33], the resistance R plays a key role in changing the damping coefficient of the electromagnetic system. For disclosing the resistance R effects, Eq. (8) is investigated separately in two modes: dissipation mode (i.e., $d=0$) and regeneration mode (i.e., $d=1$). In order to investigate the vehicle suspension performance in this study, two main transfer functions, i.e., the car body acceleration transfer function ($G_1(s)$) and the suspension travel transfer function ($G_2(s)$) are required. Substituting the values of the parameter d in Eq. (8) and assuming the parameter values in Tables 1 and 2, the two mentioned transfer functions can be calculated by use of the relationship between state space equations and transfer function.

According to the previous works, the range utilized for the resistance value is usually less than 10 Ω since it generates a suitable amount of damping for the vehicle suspension system considering ride comfort and maximum suspension travel. In this paper, the average value of 5 Ω is used as a typical value to evaluate the performance of the electromagnetic suspension system.

Table 2 The parameter values of the energy storage system

Parameter	Value
r_{s1} (Ω)	0.5
r_{s2} (Ω)	0.5
L_c (H)	0.00026
r_c (Ω)	0.16
c_u (F)	15

When $R=5$ Ω and $d=0$, then

$$G_1(s)=\frac{158.5s^5+528150.9s^4+19947942.7s^3+588193243.7s^2}{\left(\begin{array}{l}s^5+3330.4s^4+45256.5s^3+11858765.9s^2+\\19947942.7s+588193243.7\end{array}\right)}$$
$$G_2(s)=\frac{-3030.1s^3-10090184.8s^2+1.6\text{e-}7\,s+8.1\text{e-}7}{\left(\begin{array}{l}s^5+3330.4s^4+45256.5s^3+11858765.9s^2+\\19947942.7s+588193243.7\end{array}\right)} \quad (9)$$

and when $R=5$ Ω and $d=1$ then

$$G_1(s)=\frac{158.5s^6+478635.3s^5+17690516.5s^4+533035296.1s^3+5210460.4s^2}{\left(\begin{array}{l}s^6+3018.1s^5+40515.5s^4+10746630.3s^3+\\17790887.8s^2+533035296.1s+5210460.4\end{array}\right)}$$
$$G_2(s)=\frac{-3030.1s^4-9143886.4s^3-89383.1s^2+1.4\text{e-}6\,s+1.8\text{e-}8}{\left(\begin{array}{l}s^6+3018.1s^5+40515.5s^4+10746630.3s^3+\\17790887.8s^2+533035296.1s+5210460.4\end{array}\right)} \quad (10)$$

Comparison of transfer functions given by Eqs. (9) and (10) reveal that the rank of the denominator of the transfer functions increases one order in the regeneration mode.

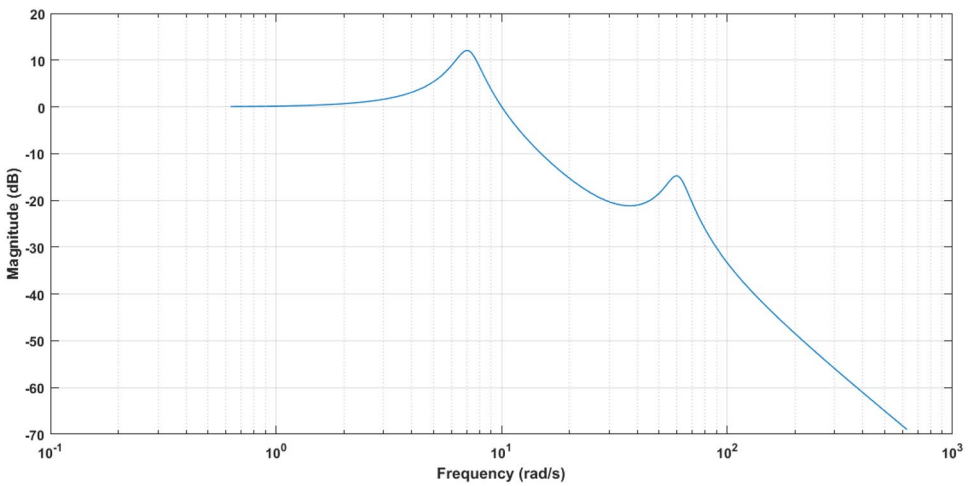

Fig. 3 Frequency response of the transfer function of the sprung mass displacement for the dissipation mode and $R=5$ Ω

Validation: To assure the accuracy of the achieved equations, the transfer function of the sprung mass displacement is first computed ($G_0(s)$) in Eq. (11)) and then its magnitude in the frequency domain is demonstrated using the data in [33] for the dissipation mode (Fig. 3). With these results, the first and second frequency of the system are found as $\omega_1 = 7.03$ rad/s and $\omega_2 = 59.67$ rad/s which is very close to those in [33] ($\omega_1 = 7.08$ rad/s and $\omega_2 = 55.19$ rad/s). The reason of the little difference is related to the modeling of the motor inductance (L_m) in this paper:

$$G_0(s) = \frac{142.7s^3 + 142855.7s^2 + 7504086.6s + 185521524.5}{s^5 + 1000.4s^4 + 19150.4s^3 + 3716635.2s^2 + 7504086.6s + 185521524.5} \tag{11}$$

Effects of *R* on the Ride Index and Maximum Suspension Travel

To study the effects of road profiles on the electromagnetic suspension system along with the energy storage system, the power spectral density (PSD) relationship between the input and output of the vehicle suspension system can be applied as follows:

$$\begin{aligned} S_1(\omega) &= \left|G_1(j\omega)\right|^2 S_g(\omega) \\ S_2(\omega) &= \left|G_2(j\omega)\right|^2 S_g(\omega) \end{aligned} \tag{12}$$

where ω is the frequency, $j = \sqrt{-1}$, S_1, S_2, and S_g are the PSD of car body acceleration, suspension travel, and road profiles, respectively. The PSD of road profiles can be expressed in the form of Eq. (13) according to ISO 8608 standard [34]:

$$S_g(\omega) = c_{sp}\frac{(\omega/2\pi)^{-n}}{V^{1-n}} \tag{13}$$

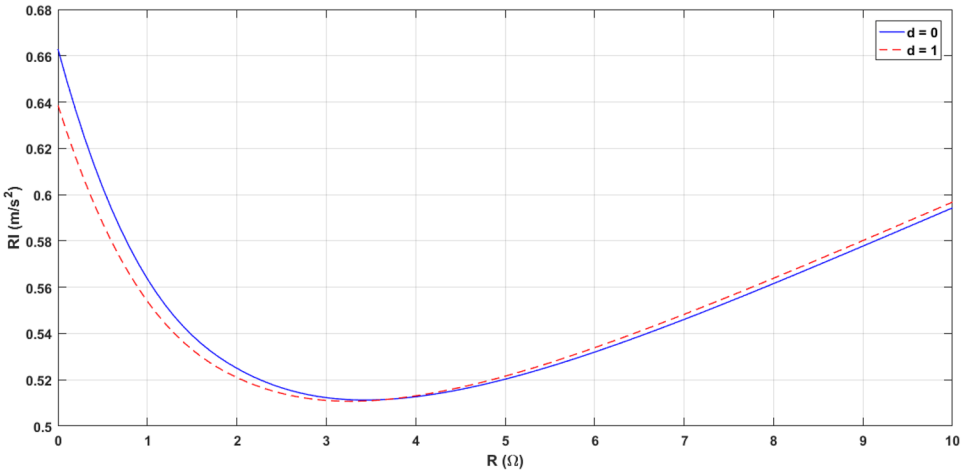

Fig. 4 Variations of the RI in terms of the *R* changes in dissipation and regeneration modes

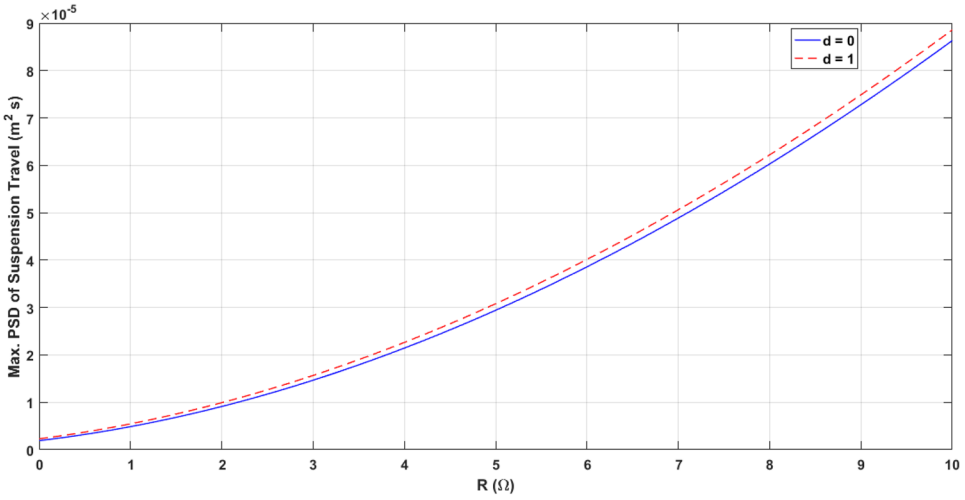

Fig. 5 Variations of the max. PSD of suspension travel in terms of the *R* changes in dissipation and regeneration modes

where c_{sp} and n are constant parameters pertinent to the type of road and V is the vehicle speed.

One of the criteria for assessing the vehicle suspension system performance is the ride index (RI) determined by means of the PSD of car body acceleration in accordance with ISO 2631-1 standard for vertical vibration [35]. Considering a typical road unevenness with $c_{sp} = 4.8 \times 10^{-7}$, $n = 2.1$, and $V = 80$ km/h, the effects of the resistance R on the vehicle suspension system performance (RI and maximum PSD of suspension travel) in two modes are illustrated in Figs. 4 and 5. Figure 4 depicts that an increase in the R value will at first lead to a decrease of the RI value and then brings a rise in this index for both dissipation and regeneration modes. In Fig. 5, it can be seen that increasing the R value leads to a rise in the maximum PSD of suspension travel in both dissipation and regeneration modes. Moreover, Fig. 4 shows that the best RI is 0.511 m/s^2 when R is 3.4 Ω in dissipation mode and the best RI is 0.510 m/s^2 when R is 3.3 Ω in regeneration mode.

Simulation Results

In order to analyze the behavior of the electromagnetic suspension system, two different types of input (y_g) are considered in this work including bump and road profile.

Bump

A typical bump as an input to the electromagnetic suspension system has been illustrated in Fig. 6. The height of this bump is equal to 5 cm. The performance of the electromagnetic suspension system including sprung mass displacement, sprung mass acceleration, and suspension travel when crossing the bump for $R = 5$ Ω is shown in Fig. 7. The maximum acceleration is 2.8 m/s^2 and the maximum suspension travel is 36 mm. One of the most significant specifications of this electromagnetic suspension system is the energy regeneration. The state of charge (SOC) of the ultracapacitor stack is demonstrated in Fig. 8. After crossing the bump, 5.5 s are approximately required that the vibration of the

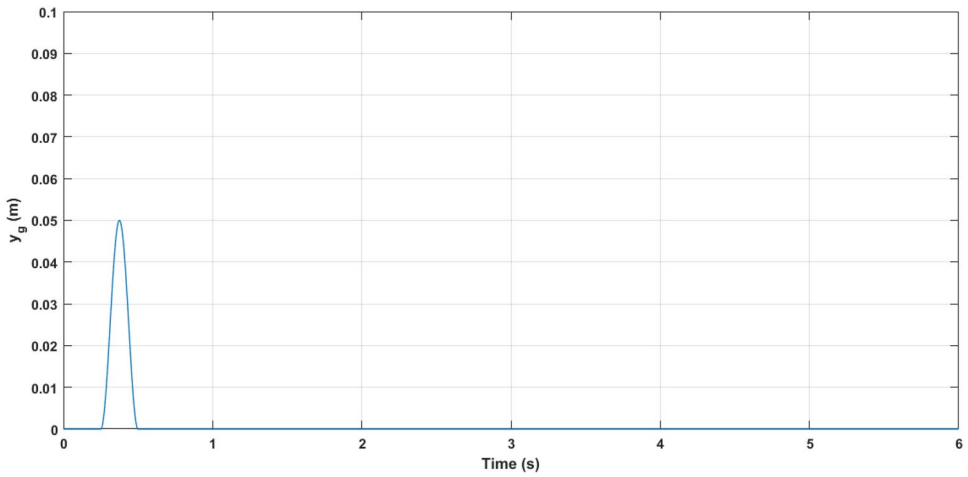

Fig. 6 A typical bump as an input for the simulation

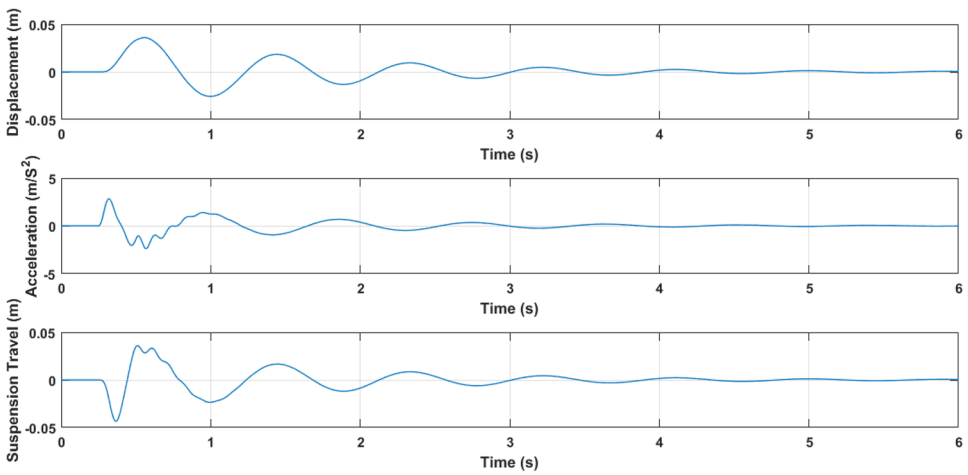

Fig. 7 Electromagnetic suspension system performance when crossing the bump

suspension system becomes zero and in this conditions, the SOC is reached to 0.21 v.

Despite the results in Figs. 7 and 8, the circumstance of the energy regeneration is not clear yet. In this regard, the parameter d can be helpful. Figure 9 represents the circumstance of the energy regeneration while crossing over the bump. As seen in this figure, the dissipation mode is occurred whenever the suspension velocity amount is zero or near to zero and energy regeneration is taken place at any time the magnitude of the suspension velocity amount is greater than zero.

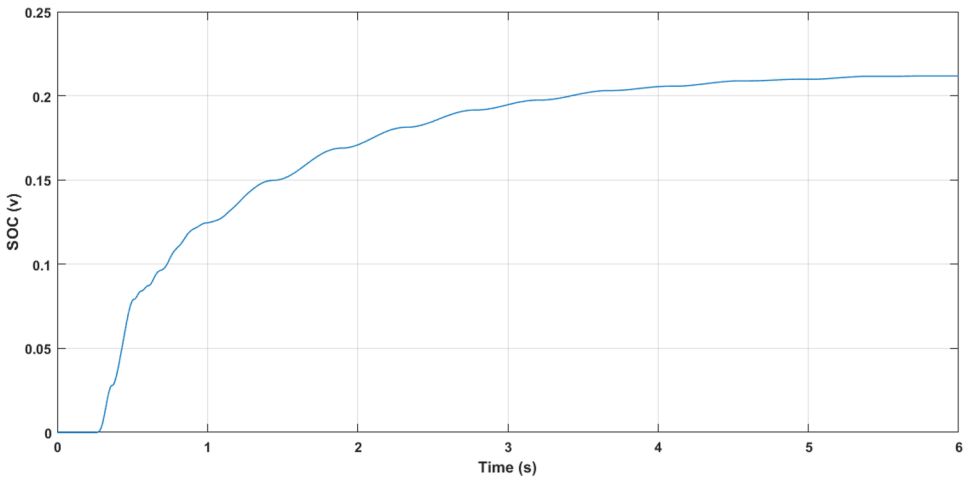

Fig. 8 SOC of the ultracapacitor stack when crossing the bump

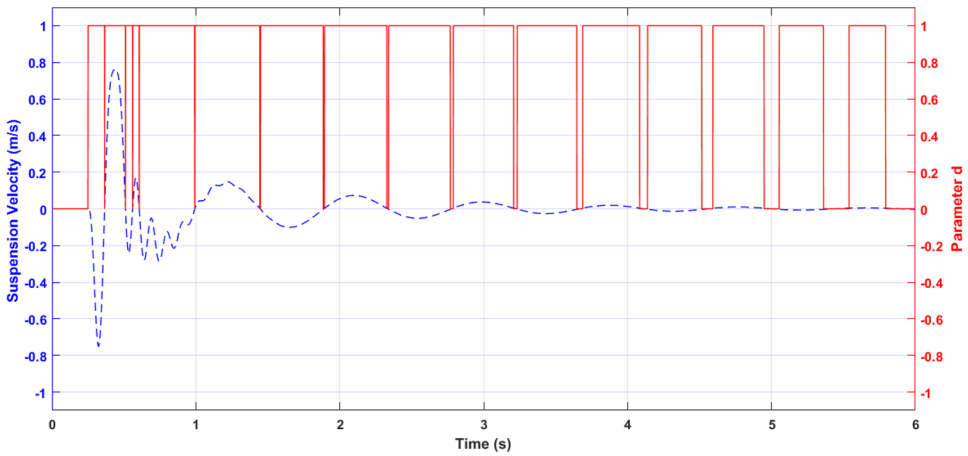

Fig. 9 Circumstance of the energy regeneration of the suspension system when crossing the bump

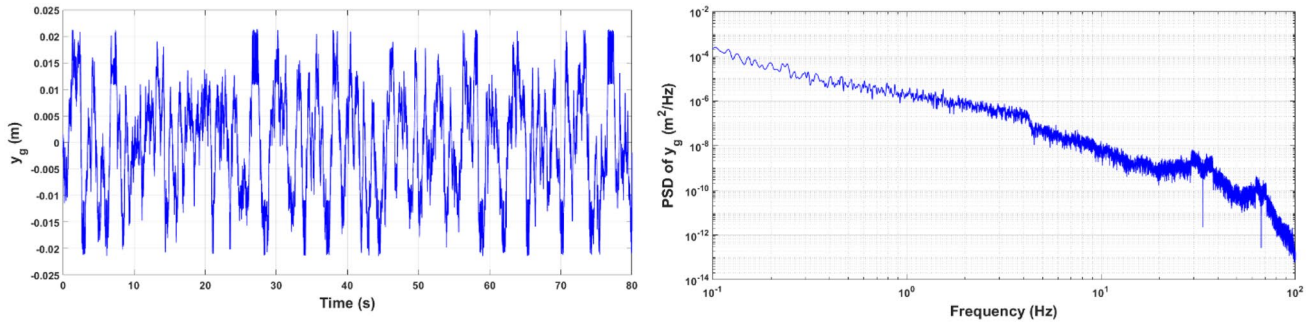

a) y_g b) PSD of the y_g

Fig. 10 Random rough road profile: **a** y_g and **b** PSD of the y_g

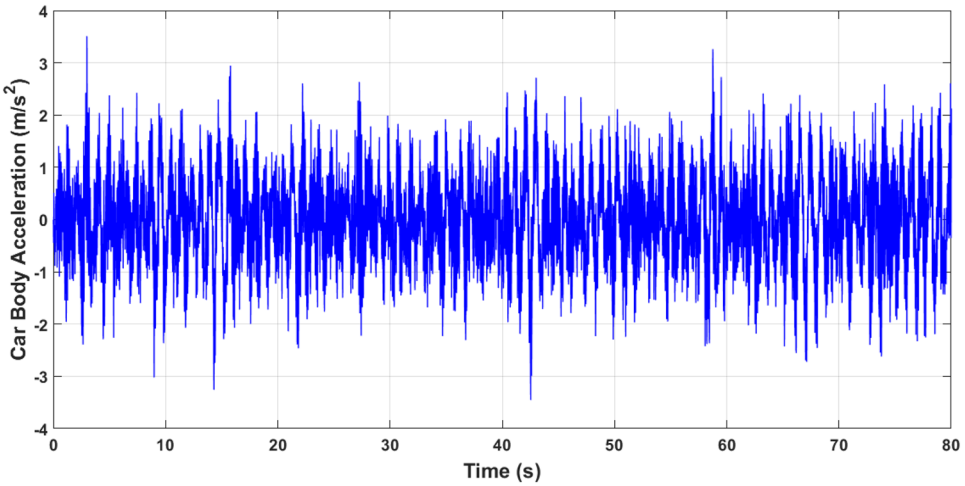

Fig. 11 Car body acceleration for the passive electromagnetic suspension system when crossing the random rough road profile

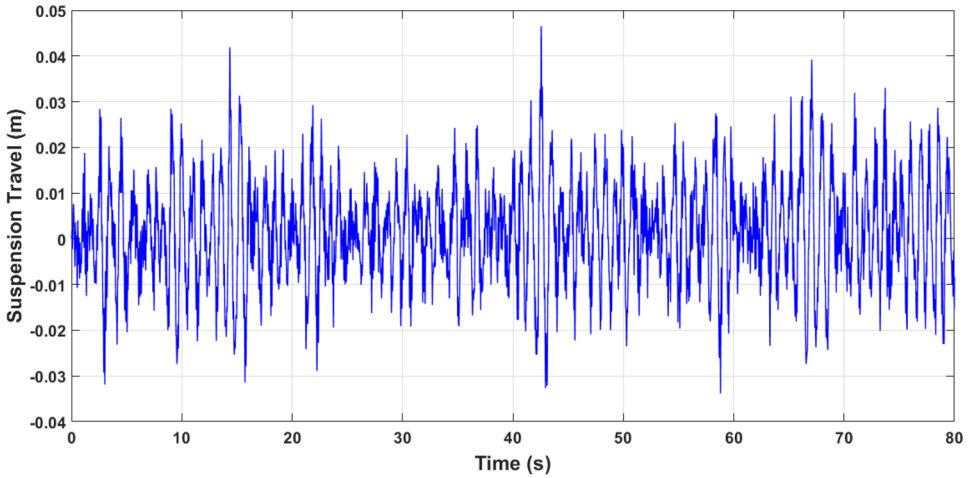

Fig. 12 Suspension travel for the passive electromagnetic suspension system when crossing the random rough road profile

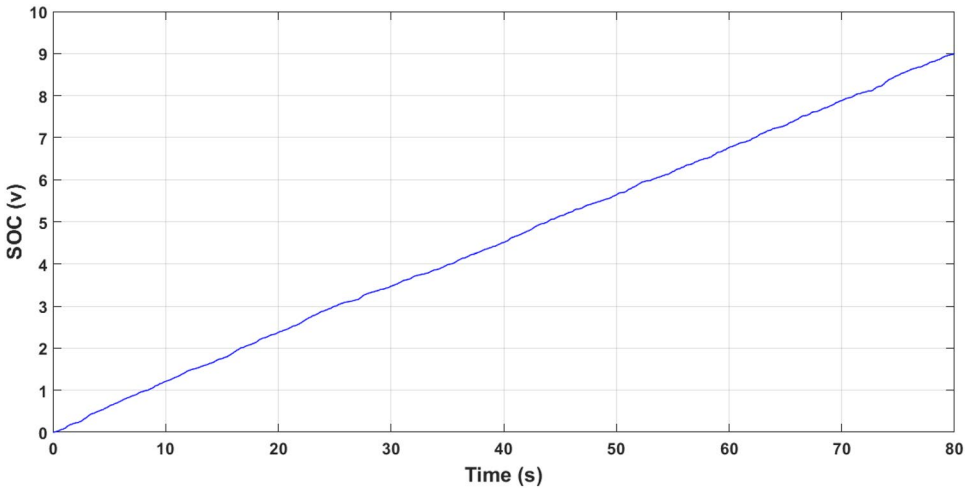

Fig. 13 SOC of the ultracapacitor stack for the passive electromagnetic suspension system when crossing the random rough road profile

Road Profile

Not only the resistance R has a key role in the electromagnetic suspension system performance and energy regeneration, but also it is able to alter the suspension system from passive state to semi-active state. In fact, the electromagnetic suspension system will be a passive system if the resistance R is constant and the electromagnetic suspension system will be a semi-active system if the resistance R is variable. In practice, there are various adjustable resistors. One of the most important types of adjustable resistors is the varistor or voltage-dependent resistor (VDR) whose resistance changes with the applied voltage. In this way, the value of the resistance is modified according to the command of the control unit. In this section, the electromagnetic suspension system behavior is investigated in two different situations, i.e., passive and semi-active states when traversing over a road with the random irregularities shown in Fig. 10a. The PSD of this road profile exposed in Fig. 10b reveals that this type of road can be approximately classified in the rough road class.

The performance of the passive electromagnetic suspension system for the mentioned road profile assuming $R=5$ Ω is depicted in Figs. 11 and 12. Furthermore, the SOC of the ultracapacitor stack is demonstrated in Fig. 13. Applying Eq. (14), the energy saving per time in the ultracapacitor stack can be estimated. This value is equal to 7.6 J/s for the passive electromagnetic suspension system. In Eq. (14), t is the time:

$$e_t = \frac{1}{2}c_u\left(\Delta v_u^2\right)/(\Delta t) \tag{14}$$

For better performance, the semi-active electromagnetic suspension system is suggested. If R is constant, it leads to a passive electromagnetic suspension system and if R is variable, it causes a semi-active electromagnetic suspension system. Several semi-active control strategies have been proposed by many researchers. This work employs the continuous skyhook control strategy which can be expressed as [36]

$$R = \begin{cases} \min\left\{R_{\max}, \max\left\{R_c, \frac{\dot{y}_s}{(\dot{y}_s-\dot{y}_u)}R_{\min}\right\}\right\} & \dot{y}_s\left(\dot{y}_s-\dot{y}_u\right) \geq 0 \\ R_{\max} & \dot{y}_s\left(\dot{y}_s-\dot{y}_u\right) < 0 \end{cases} \tag{15}$$

where R_c is the constant value determined by the designer and considering $R_{\min} < R_c < R_{\max}$.In essence, the skyhook control strategy adds more damping to the sprung mass, and is ideal if the primary goal is to isolate the sprung mass from the base excitations. Equation (15) implies that when the relative velocity of the suspension system and the absolute velocity of the sprung mass have the same sign (both in the same direction), a high damping force is desired (i.e., a value close to R_c). Otherwise, small damping force is required (i.e., maximum R).

Table 3 The simulation results for the passive and semi-active electromagnetic suspension system when crossing the random rough road profile

	RI (m/s^2)	Max. suspension travel (mm)	Stored energy (J/s)
Passive system	0.680	46.5	7.6
Semi-active system	0.645	40	8.6
Improvement (%)	5	14	13

$R_{\min}$ is equal to zero and $R_{\max}$ is supposed to be 5 Ω so as to contrast the performance of the semi-active electromagnetic suspension system with the passive electromagnetic suspension system. Here, a method is offered to adjust the R_c value using the results in Fig. 4. Actually, it is proposed that the R_c value is considered to be 3.4 Ω in dissipation mode and 3.3 Ω in regeneration mode. Afterwards, the simulation is performed by the use of the above assumptions. In this situation, the energy saving per time in the ultracapacitor stack is equal to 8.6 J/s. The performance and energy regeneration of the passive and semi-active electromagnetic suspension systems have been compared in Table 3. It can be deduced from Table 3 that the semi-active electromagnetic suspension system has better performance in comparison with the passive electromagnetic suspension system while the energy regeneration of the semi-active electromagnetic suspension system is more than that of the passive electromagnetic suspension system.

Conclusion

This paper dealt with the electromagnetic suspension system consisting of a permanent-magnet DC motor, a ball screw, and a nut along with the energy storage system including a unidirectional converter, a full wave rectifier, and an ultracapacitor stack. The state space equations of the mentioned system were developed by considering some of non-idealities that affect the performance of the converter in the energy storage system. The effects of resistance R (design parameter) in the energy storage system on the performance of the vehicle suspension system were investigated for the dissipation and regeneration modes in detail. The obtained results are expressed as follows:

– The denominator rank of the transfer functions increases one order in the regeneration mode.

- – The best RI occurs when R is 3.4 Ω in dissipation mode and the best RI happens when R is 3.3 Ω in regeneration mode.
- Assuming $R = 5$ Ω, the SOC of the ultracapacitor stack reaches 0.21 v after passing through the bump. It also takes approximately 5.5 s for the suspension vibration to disappear.
- The energy regeneration investigation of the passive electromagnetic suspension system while passing over the bump reveals that the dissipation mode occurs whenever the suspension velocity amount is zero or close to zero, and whenever the magnitude of the suspension velocity amount is greater than zero, energy is regenerated.
- The electromagnetic damper can play a semi-active actuator role if R is considered as a variable resistance.
- The semi-active electromagnetic suspension system designed using the continuous skyhook control strategy outperforms the passive electromagnetic suspension system in terms of RI and maximum suspension travel when traversing a random rough road profile. Besides, the amount of energy stored by the semi-active system is 13% more than the passive system. The stored energy of the semi-active and passive suspension system is equal to 8.6 J/s and 7.6 J/s, respectively.

Funding The author did not receive support from any organization for the submitted work.

Declarations

Conflict of Interest On behalf of all the authors, the corresponding author states that there is no conflict of interest.

References

1. Zhang R, Wang X, Liu Z (2017) A novel regenerative shock absorber with a speed doubling mechanism and its Monte Carlo simulation. J Sound Vib 417:260–276. https://doi.org/10.1016/j.jsv.2017.12.017
2. Tang X, Lin T, Zuo L (2014) Design and optimization of a tubular linear electromagnetic vibration energy harvester. IEEE/ASME Trans Mechatron 19(2):615–622. https://doi.org/10.1109/TMECH.2013.2249666
3. Gysen BLJ, van der Sande TPJ, Paulides JJH, Lomonova EA (2011) Efficiency of a regenerative direct-drive electromagnetic active suspension. IEEE Trans Veh Technol 60(4):1384–1393. https://doi.org/10.1109/TVT.2011.2131160
4. Kawamoto Y, Suda Y, Inoue H, Kondo T (2008) Electro-mechanical suspension system considering energy consumption and vehicle manoeuvre. Veh Syst Dyn 46:1053–1063
5. Xie L, Li J, Cai S, Li X (2017) Electromagnetic energy-harvesting damper with multiple independently-controlled transducers: on-demand damping and optimal energy regeneration. IEEE/ASME Trans Mechatron 22:2705–2713. https://doi.org/10.1109/TMECH.2017.2758783
6. Roshan YM, Maravandi A, Moallem M (2015) Power electronics control of an energy regenerative mechatronic damper. IEEE Trans Ind Electron 62(5):3052–3060. https://doi.org/10.1109/TIE.2015.2392714
7. Zhang Z, Zhang X, Chen W, Rasim Y, Salman W, Pan H et al (2016) A high-efficiency energy regenerative shock absorber using supercapacitors for renewable energy applications in range extended electric vehicle. Appl Energy 178:177–188. https://doi.org/10.1016/j.apenergy.2016.06.054
8. Salman W, Qi L, Zhu X, Pan H, Zhang X, Bano S, Zhang Z et al (2018) A high-efficiency energy regenerative shock absorber using helical gears for powering low-wattage electrical device of electric vehicles. Energy 159:361–372. https://doi.org/10.1016/j.energy.2018.06.152
9. Liu Y, Xu L, Zuo L (2017) Design, modeling, lab, and field tests of a mechanical-motion-rectifier-based energy harvester using a ball-screw mechanism. IEEE/ASME Trans Mechatron 22(5):1933–1943. https://doi.org/10.1109/TMECH.2017.2700485
10. Zhang R, Wang X, Shami EA, John S, Zuo L et al (2018) A novel indirect-drive regenerative shock absorber for energy harvesting and comparison with a conventional direct-drive regenerative shock absorber. Appl Energy 229:111–127. https://doi.org/10.1016/j.apenergy.2018.07.096
11. Galluzzi R, Xu Y, Amati N, Tonoli A (2018) Optimized design and characterization of motor-pump unit for energy-regenerative shock absorbers. Appl Energy 210:16–27. https://doi.org/10.1016/j.apenergy.2017.10.100
12. Zhang Y, Chen H, Guo K, Zhang X, Lic SE (2017) Electro-hydraulic damper for energy harvesting suspension: Modeling, prototyping and experimental validation. Appl Energy 199:1–12. https://doi.org/10.1016/j.apenergy.2017.04.085
13. Fang ZG, Guo XX, Xu L, Zhang H (2013) Experimental study of damping and energy regeneration characteristics of a hydraulic electromagnetic shock absorber. Adv In Mech Eng 5:943528. https://doi.org/10.1155/2013/943528
14. Abdelkareem MAA, Xu L, Ali MKA, El-Daly ARBM, Hassan MA, Elagouz A, Bo Y (2019) Analysis of the prospective vibrational energy harvesting of heavy-duty truck suspensions: a simulation approach. Energy 173:332–351. https://doi.org/10.1016/j.energy.2019.02.060
15. Abdelkareem MAA, Xu L, Ali MKA, Elagouz A, Mi J, Guo S, Liu Y, Zuo L (2018) Vibration energy harvesting in automotive suspension system: a detailed review. Appl Energy 229:672–699. https://doi.org/10.1016/j.apenergy.2018.08.030
16. Ruichen PZ, Gao WJ (2019) A comprehensive review on regenerative shock absorber systems. J Vib Eng Technol. https://doi.org/10.1007/s42417-019-00101-8
17. Marzougui H, Kadri A, Martin J-P, Amari M, Pierfederici S, Bacha F (2019) Implementation of energy management strategy of hybrid power source for electrical vehicle. Energy Convers Manag 195:830–843
18. Schneuwly A (2005) Charging ahead (ultracapacitor technology and applications). Power Eng 19(1):34–37
19. Zhao H, Wu Q, Hu S, Xu H, Rasmussen CN (2015) Review of energy storage system for wind power integration support. Appl Energy 137:545–553
20. Luo X, Wang J, Dooner M, Clarke J (2015) Overview of current development in electrical energy storage technologies and the application potential in power system operation. Appl Energy 137:511–536
21. Miller JM (2011) Ultracapacitor applications (energy engineering). The Institution of Engineering and Technology, London

22. Ahmed OA, Bleijs JAM (2015) An overview of DC–DC converter topologies for fuel cell-ultracapacitor hybrid distribution system. Renew Sustain Energy Rev 42:609–626
23. Ahmed OA, Bleijs JAM (2013) Power flow control methods for an ultracapacitor bidirectional converter in DC microgrids: a comparative study. Renew Sustain Energy Rev 26:727–738
24. Jing W, Lai CH, Wong SHW, Wong MLD (2016) Battery-supercapacitor hybrid energy storage system in standalone dc microgrids: a review. IET Renew Power Gener 11(4):461–469
25. Kuperman A, Aharon I (2011) Battery–ultracapacitor hybrids for pulsed current loads: a review. Renew Sustain Energy Rev 15(2):981–992
26. Zhao C, Yin H, Ma C (2019) Equivalent series resistance-based real-time control of battery-ultracapacitor hybrid energy storage systems. IEEE Trans Ind Electron 67(3):1999–2008
27. Amal S, Chacko RV, Sreedevi M, Mineeshma G, Vishnu V (2016) Modelling of ultracapacitor and power management strategy for the parallel operation of ultracapacitor and battery in electric vehicle configuration. In: IEEE International Conference on Power Electronics, Drives and Energy Systems (PEDES), pp 1–6
28. Manla E, Mandic G, Nasiri A (2014) Development of an electrical model for lithium ion ultracapacitors, IEEE. J Emerg Sel Top Power Electron 3(2):395–404
29. Bharti A, Kumar G, Ahmed M, Gupta P, Bocchetta R, Adalati R, Chandra R, Kumar Y (2021) Theories and models of supercapacitors with recent advancements: impact and interpretations. Nano Express 2:022004. https://doi.org/10.1088/2632-959X/abf8c2
30. Navarro G, Torres J, Blanco M, Najera J, Santos-Herran M, Lafoz M (2021) Present and future of supercapacitor technology applied to powertrains, renewable generation and grid connection applications. Energies 14:3060. https://doi.org/10.3390/en14113060
31. Naresh P, Sai-Vinay-Kishore N, Seshadri-Sravan-Kumar V (2021) Mathematical modeling and stability analysis of an ultracapacitor based energy storage system considering non-idealities. J Energy Storage 33:102112. https://doi.org/10.1016/j.est.2020.102112
32. Kawamoto Y, Suda Y, Inoue H, Kondo T (2007) Modeling of electromagnetic damper for automobile suspension. J Syst Des Dyn 1:524–535
33. Montazeri-Gh M, Kavianipour O (2012) Investigation of the passive electromagnetic damper. Acta Mech 223:2633–2646. https://doi.org/10.1007/s00707-012-0735-8
34. ISO (1995) Mechanical vibration—road surface profiles—reporting of measured data. ISO, Geneva, p 8608
35. ISO (1997) Mechanical vibration and shock—evaluation of human exposure to whole-body vibration. ISO, Geneva, p 2631
36. Shamsi A, Choupani N (2008) Continuous and discontinuous shock absorber control through skyhook strategy in semi-active suspension system (4DOF model). Eng Technol 41:745–749

Publisher's Note Springer Nature remains neutral with regard to jurisdictional claims in published maps and institutional affiliations.

Springer Nature or its licensor holds exclusive rights to this article under a publishing agreement with the author(s) or other rightsholder(s); author self-archiving of the accepted manuscript version of this article is solely governed by the terms of such publishing agreement and applicable law.